Volume 9
Number 4
21 February 2025
Pages 895–1132

Sustainable Energy & Fuels

Interdisciplinary research for the development of sustainable energy technologies

rsc.li/sustainable-energy

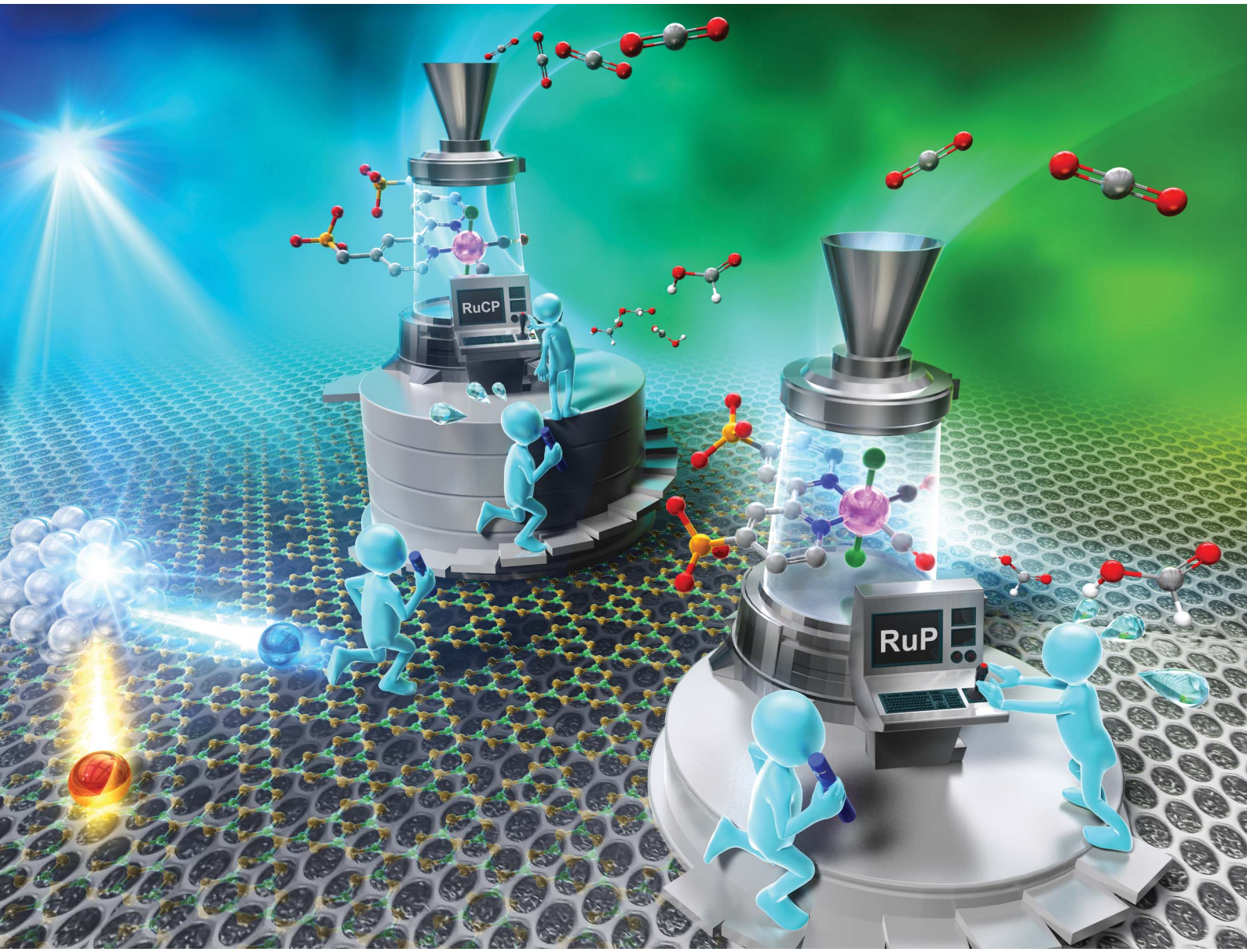

ISSN 2398-4902

ROYAL SOCIETY OF CHEMISTRY

PAPER

Guigang Zhang, Kazuhiko Maeda *et al.*

Light-intensity dependence of visible-light CO_2 reduction over Ru(II)-complex/Ag/polymeric carbon nitride hybrid photocatalysts

Sustainable Energy & Fuels

ROYAL SOCIETY OF CHEMISTRY

PAPER

View Article Online
View Journal | View Issue

Cite this: *Sustainable Energy Fuels*, 2025, **9**, 947

Light-intensity dependence of visible-light CO_2 reduction over Ru(II)-complex/Ag/polymeric carbon nitride hybrid photocatalysts†

Ryuichi Nakada,[a] Chao Zhang,[b] Jo Onodera,[a] Toshiya Tanaka,[a] Megumi Okazaki,[a] Guigang Zhang *[b] and Kazuhiko Maeda *[ac]

Received 25th October 2024
Accepted 30th November 2024

DOI: 10.1039/d4se01488j

rsc.li/sustainable-energy

Photocatalytic CO_2 reduction over Ru(II)-complex/Ag/polymeric carbon nitride (PCN) was studied with respect to light intensity and the type of Ru(II) complex. In experiments using two different Ru(II) complex cocatalysts, the reduction potential of the Ru complex was found to balance efficient CO_2 reduction on the Ru complex with electron transfer from Ag/PCN. This balance avoided the formation of H_2 as a byproduct, minimized charge accumulation in Ag/PCN, and maximized the apparent quantum yield for CO_2-to-HCOOH conversion.

Introduction

CO_2 is an important source of C1 chemicals in organic synthesis[1–3] and biosynthesis.[4] Photocatalytic CO_2 reduction is another promising approach because it produces value-added chemicals (*e.g.*, HCOOH and CO) using inexhaustible sunlight. Metal-complex (photo)catalysts are highly active toward the reduction of CO_2 with high selectivity. However, the photo-oxidative ability of the metal-complex photocatalysts is insufficient to achieve artificial photosynthetic reactions using water as an electron donor. By contrast, semiconductor photocatalysts generally exhibit good photo-oxidation power but low selectivity for CO_2 reduction. To further exploit the advantages of both metal-complex and semiconductor photocatalysts while minimizing their weakness, researchers have intensively studied metal-complex/semiconductor hybrid photocatalysts over the past decade.[5–8]

One of the most studied metal-complex/semiconductor hybrid photocatalysts is based on a polymeric carbon nitride (PCN) absorber modified with a mononuclear metal complex cocatalyst (Scheme 1).[9–16] For example, PCNs functionalized with *trans*(Cl)-[Ru^{II}(bpyX_2)(CO)$_2$Cl$_2$] (bpyX_2 = 2,2′-bipyridine with substituents X in the 4-positions; X = PO_3H_2, $CH_2PO_3H_2$), represented as **RuP** and **RuCP** hereafter, can reduce CO_2 into HCOOH with 80–90% selectivity under visible light in the presence of triethanolamine (TEOA) as an electron donor.[9,11] The activity of the Ru(II) complex/PCN hybrid is further enhanced through modification of the PCN component with Ag nanoparticles, which promote charge separation followed by electron transfer to the Ru complex.[17,18]

For heterogeneous photocatalysts, especially those for water splitting or H_2 evolution reactions, investigating the dependence of the photocatalytic activity on the light intensity has been shown to provide mechanistic insights into the bottlenecks in the associated photocatalytic reactions.[19–24] By contrast, such studies involving heterogeneous photocatalysts for CO_2 reduction are rare. In the conversion of CO_2 to CH_4 by a P25 TiO_2 photocatalyst, the rate of CH_4 formation has been reported to increase in proportion to the square root of the light intensity; however, the origin of the CH_4 remains unclear because of a lack of $^{13}CO_2$ isotope experiments.[25] Shangguan

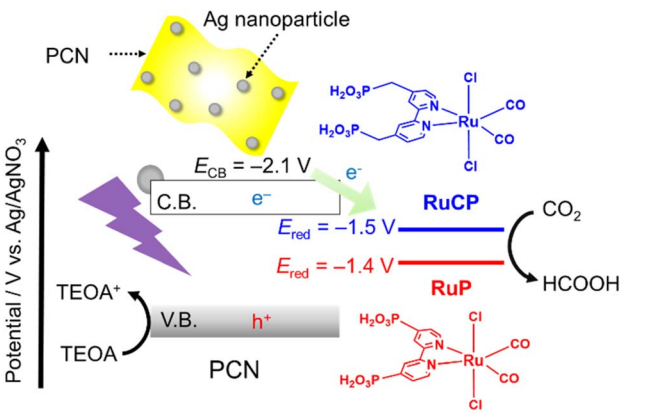

Scheme 1 Schematic of photocatalytic CO_2 reduction over Ru complex/Ag/PCN.

[a]*Department of Chemistry, School of Science, Institute of Science Tokyo, 2-12-1-NE-2 Ookayama, Meguro-ku, Tokyo 152-8550, Japan. E-mail: maeda@chem.sci.isct.ac.jp*

[b]*State Key Laboratory of Photocatalysis on Energy and Environment, College of Chemistry, Fuzhou University, Fuzhou 350108, P. R. China. E-mail: guigang.zhang@fzu.edu.cn*

[c]*Research Center for Autonomous Systems Materialogy (ASMat), Institute of Science Tokyo, 4259 Nagatsuta-cho, Midori-ku, Yokohama, Kanagawa 226-8501, Japan*

† Electronic supplementary information (ESI) available: Additional characterization and reaction data. See DOI: https://doi.org/10.1039/d4se01488j

et al. have reported that Au nanoparticles photocatalyze the reduction of CO_2 to CO with the aid of H_2O as a result of interband transitions of Au driven by visible light and that the rate of CO production increases almost linearly with increasing light intensity.[26] For homogeneous systems, Ishida *et al.* have reported the light-intensity dependence of photocatalytic CO_2 reduction using a mixed system of *trans*(Cl)-Ru(bpy)$(CO)_2Cl_2$ and $[Ru(bpy)_3]^{2+}$ as a catalyst and a photosensitizer, respectively, with the aid of 1-benzyl-1,4-dihydronicotinamide as an electron donor.[27] According to their study, the ratio of CO/HCOOH products increased with increasing light intensity. Because some derivatives of *trans*(Cl)-Ru(bpy)$(CO)_2Cl_2$ have been used as active molecular cocatalysts for CO_2 reduction with PCN, studying the light-intensity dependence of visible-light CO_2 reduction over Ru complex/PCN hybrid photocatalysts, which has not been reported thus far, would be intriguing.

In the present study, we focused on the three-component hybrid photocatalysts **RuP** (or **RuCP**)/Ag/PCN and investigated the light-intensity dependence of the CO_2 photoreduction quantum yield and the product selectivity. The significant effect of the reduction potential of the Ru complexes on CO_2 photoreduction quantum yield and product selectivity with respect to the incident light intensity is reported.

Results and discussion

PCN and Ag/PCN were synthesized according to a previously reported method.[17] Some essential characterization results, including the results of X-ray diffraction, UV-visible diffuse-reflectance spectroscopy, electron microscopy, and X-ray photoelectron spectroscopy experiments, are shown in the ESI (Fig. S1–S3†). The syntheses of **RuP** and **RuCP** were conducted in accordance with a previous report.[28] As reported elsewhere, PCN absorbs visible light with wavelengths as long as ~420 nm,[17] whereas **RuP** and **RuCP** basically do not absorb visible light.[11] The detailed procedures and materials characterization results can be found in the corresponding literature.

First, the CO_2 reduction reaction over **RuP**/Ag/PCN was carried out in a CO_2-saturated mixed solution of *N*,*N*-dimethylacetamide (DMA) and TEOA (4 : 1 v/v) under 400 nm monochromatized light with different light-intensity conditions. In this work, the wavelength of 400 nm was employed because PCN absorbs 400 nm light, while **RuP** and **RuCP** do not.[11] Here, the apparent quantum yield (AQY) for HCOOH generation was calculated using an equation adopted from a previous report:[24]

$$\mathrm{AQY}(\%) = \frac{A \times \text{number of product molecules}}{\text{number of incident photons}} \times 100$$

where A represents the coefficient of the reaction (here, $A = 2$).

$$\text{Number of product molecules } [\mathrm{h^{-1}}] = v[\mu\mathrm{mol\ h^{-1}}] \times N_A\ [\mathrm{mol^{-1}}] \times 10^{-6}$$

where v and N_A are the rate of reaction rate and Avogadro's constant, respectively.

$$\text{Number of incident photons } [\mathrm{h^{-1}}] = \frac{\lambda\ [\mathrm{m}] \times I\ [\mathrm{mW\ cm^{-2}}] \times S\ [\mathrm{cm^2}]}{h\ [\mathrm{J\ s}] \times c\ [\mathrm{m\ s^{-1}}]} \times 3.6$$

where I, S, h, and c are the wavelength of the incident light, the light intensity (measured by a spectrophotometer; LS-100, Eko Instruments), the irradiation area, Planck's constant, and the speed of light, respectively. In this research, the irradiation area was fixed at 4.4 cm^2, and the light intensity was controlled by adjusting the output power of the Xe lamp. The maximum light intensity employed in this work was ~10 mW cm^{-2} due to the power limit of the light source.

Fig. 1a shows the AQY for visible-light-driven HCOOH production over **RuP**/Ag/PCN as a function of the incident-light intensity. The AQY recorded in the light-intensity range ≤5.0 mW cm^{-2} was ~2.5% and almost independent of the light intensity. However, the AQY decreased sharply as the light intensity was increased beyond 5.0 mW cm^{-2}. The results confirmed that the turnover number for HCOOH formation (TON_{HCOOH}) was much larger than 1 in all cases (Table S1†), indicating that HCOOH formation was catalytically cycled. In previous work, we demonstrated that the generation of HCOOH over the **RuP**/Ag/PCN hybrid photocatalyst is stable until the TON_{HCOOH} reaches ~5800.[17] In the present work, the recorded TON_{HCOOH} was at most ~300 because the reactions were conducted under relatively low-intensity visible light for 2 h. Therefore, the degradation of the activity of the **RuP**/Ag/PCN hybrid photocatalyst during the CO_2 reduction can be regarded as negligible.

The relationship between the rate of HCOOH production (v_{HCOOH}) and the incident-light intensity (I) is displayed in Fig. 1b.

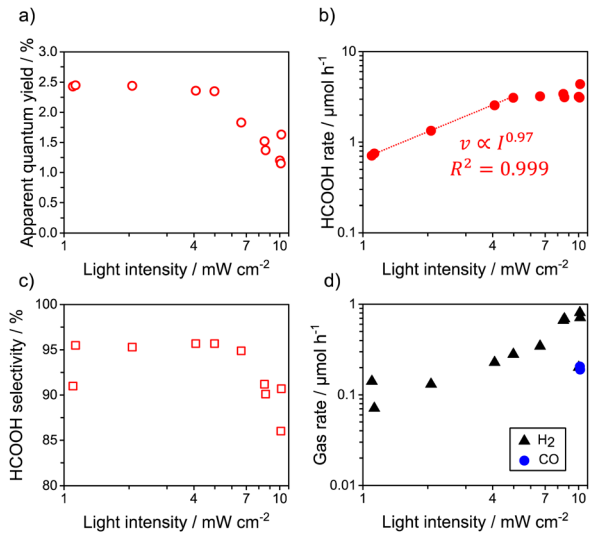

Fig. 1 (a) Apparent quantum yield, (b) HCOOH production rate, (c) HCOOH selectivity, and (d) rate of gas-phase product formation from **RuP**/Ag/PCN as function of the incident-light intensity. Reaction conditions: catalyst, 14 mg; reactant solution, DMA : TEOA mixture solvent (4 : 1 v/v, 14 mL); wavelength of light, 400 nm, Ag: 2.0 wt%, adsorbed amount of **RuP**: 2 μmol g^{-1}.

The data plot in lower-light-intensity regions could be fitted by the equation:

$$v_{HCOOH} = aI^b$$

The HCOOH production rate (v_{HCOOH}) was almost proportional to the light intensity ($I^{0.97}$) in the region ≤5.0 mW cm^{-2} (Table S2†). However, in the region >5.0 mW cm^{-2}, the HCOOH rate remained almost unchanged. The HCOOH selectivity was also found to decrease (Fig. 1c), similar to the AQY results. The decrease in the HCOOH selectivity is attributed to the reaction order for the main gas-phase byproduct, H_2, not changing with increasing light intensity (Fig. 1d). The corresponding H_2 evolution AQY was ~0.2%, independent of the light intensity.

The reduction of CO_2 over **RuCP**/Ag/PCN was similarly tested; the results are shown in Fig. 2 and Table S3.† Unlike the AQY achieved with **RuP**/Ag/PCN, that achieved with **RuCP**/Ag/PCN decreased gradually with increasing light intensity (Fig. 2a). From Fig. 2b, the reaction order for light the intensity of **RuCP**/Ag/PCN was determined to be 0.72, which was lower than that for the **RuP** loading in the light-intensity regime of ≤5.0 mW cm^{-2} (0.97). The CO_2-to-HCOOH selectivity was 90–95% irrespective of the light intensity (Fig. 2c). The rate of H_2 byproduct formation tended to increase with increasing light intensity (Fig. 2d). No CO was detected in the products generated over **RuCP**/Ag/PCN. The trend of CO_2 reduction selectivity for **RuCP**/Ag/PCN with respect to light intensity was thus different from that for **RuP**/Ag/PCN.

The results thus demonstrated that the behavior of Ru complex/Ag/PCN ternary hybrid photocatalysts toward CO_2 reduction was dependent on the type of the Ru complex and the incident light intensity. In the light-intensity range ≤5.0 mW cm^{-2}, **RuP**/Ag/PCN gave a HCOOH generation reaction order close to unity with respect to light intensity (Fig. 1b). This result indicates that the overall reaction rate was determined by light absorption of the PCN component, as reported for other heterogeneous photocatalysts for water splitting.[19,21,23,24] Of course, at least ~90% of the photogenerated carriers were unused for the surface reaction because of recombination. When the light intensity was greater than 5.0 mW cm^{-2}, light absorption by PCN was no longer the rate-determining step. Increasing the light intensity above 5.0 mW cm^{-2} resulted in a monotonic decrease in the AQY for HCOOH generation and a concomitant increase in H_2 evolution, suggesting that there is a critical CO_2-reduction bottleneck other than light absorption and charge migration in PCN.

The **RuCP**/Ag/PCN photocatalyst showed a different light-intensity dependence of photocatalytic CO_2 reduction, giving a dependence of $I^{\sim 0.7}$ in the entire examined light-intensity range (Fig. 2b). We speculate that the difference in the light-intensity dependence of CO_2 reduction originates from the difference in the reduction potential of the Ru complexes. The reduction potential of **RuCP** has been shown to be 0.1 V more negative than that of **RuP**.[11] Therefore, compared with **RuP**, **RuCP** exhibits greater difficulty in receiving an electron from Ag/PCN from the viewpoint of thermodynamics, but has a higher driving force for CO_2 reduction. It should be also noted that the catalytic Ru center in **RuCP** is more distant from Ag/PCN than **RuP** because of the presence of methylene spacer, which would adversely affect the efficiency of electron transfer.[29]

That is, **RuP** is disadvantageous over **RuCP** in terms of the driving force for CO_2 reduction, which could become the rate-determining step under high-light-intensity conditions. For a homogeneous CO_2 photoreduction system composed of *trans*-(Cl)-[Ru(5,5′-diamide-2,2′-bipyridine)(CO)$_2$Cl$_2$]-type complex catalysts and [Ru(bpy)$_3$]$^{2+}$ as a photosensitizer, Ishida *et al.* have reported that the turnover frequency for CO_2 reduction increases exponentially with a negative shift of the potential of the catalyst complex until the potential reaches the reduction potential of [Ru(bpy)$_3$]$^{2+}$.[30] Notably, the rate of H_2 byproduct formation during the CO_2 reduction over **RuP**/Ag/PCN increased with a reaction order of ~0.9. Because the Ag on the PCN can act as a H_2 evolution cocatalyst,[31] we speculate that the electrons in Ag/PCN, which had nowhere else to go because **RuP** no longer functioned properly, participated in H_2 generation on the loaded Ag. We also note that Ag/PCN alone (*i.e.*, without **RuP** or **RuCP**) gave AQYs of ~0.2% and <0.1% for H_2 and HCOOH generation, respectively, at 5.0 mW cm^{-2}. That is, the selectivity of Ag/PCN to HCOOH was at most ~35%, which is much lower than the selectivities recorded using the **RuP**- or **RuCP**-loaded analogues. Thus, when the outlet for CO_2 reduction is blocked, the HCOOH generation AQY decreases drastically, whereas H_2 production becomes relatively dominant (although the H_2-evolution AQY remains approximately the same).

Because of the greater CO_2 reduction driving force for **RuCP**, the CO_2 reduction process on the **RuCP** is not a critical bottleneck. However, a certain degree of charge accumulation in Ag/PCN occurred even in combination with **RuCP** because

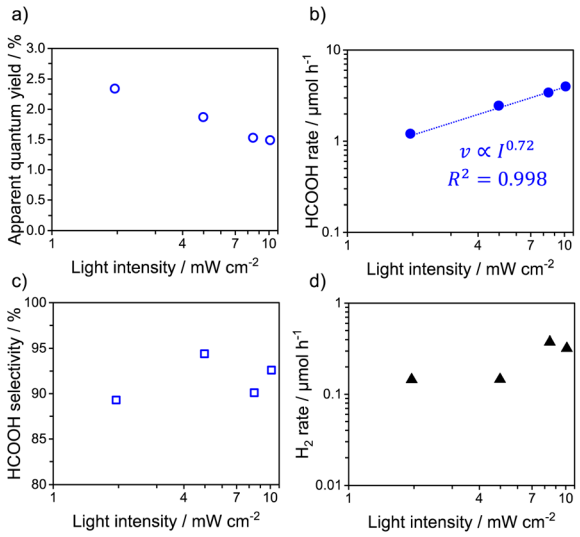

Fig. 2 (a) Apparent quantum yield, (b) HCOOH production rate, (c) HCOOH selectivity, and (d) rate of gas-phase product formation from **RuCP**/Ag/PCN as function of the incident-light intensity. Reaction conditions: catalyst, 14 mg; reactant solution, DMA : TEOA mixture solvent (4 : 1 v/v, 14 mL); wavelength of light, 400 nm, Ag: 2.0 wt%, adsorbed amount of **RuCP**: 2 μmol g^{-1}.

electron transfer from Ag/PCN to **RuCP** is less efficient than that to **RuP**,[11] as previously mentioned. That is, the greater the difficulty of the terminal reduction reaction, the more pronounced the charge accumulation in the PCN and the lower the reaction quantum yield.

In this regard, we conducted the H_2 evolution reaction under the same reaction conditions as CO_2 reduction but with PCN modified with a Pt cocatalyst, which is one of the most effective promoters of H_2 evolution for PCN.[32] The characterization data for Pt/PCN are included in Fig. S1–S3.† Fig. S4† shows the H_2 evolution AQY and rate as functions of the light intensity. As expected, nearly twofold higher AQY (4.5–5.5%) was obtained compared with that recorded in CO_2 reduction (~2.5% at most, see Fig. 1a and 2a). The Pt/PCN gave a H_2 evolution reaction order of ~0.8 for light intensity, which was higher than the CO_2 reduction order recorded using **RuCP**/Ag/PCN (~0.7). From this result, one might expect that further improving the activity for CO_2 reduction over metal-complex/PCN hybrid photocatalysts could be realized if a suitable metal-complex cocatalyst with a more negative reduction potential not exceeding the conduction-band minimum of PCN is developed.

Conclusions

In conclusion, we observed unique light-intensity-dependent CO_2 reduction over Ru complex/Ag/PCN hybrid photocatalysts under 400 nm visible light. Using **RuP**, which features a more positive reduction potential, we found two operational regimes: One regime is $\leq$5.0 mW cm^{-2}, where the HCOOH production rate increased in proportion with the light intensity while a high CO_2-to-HCOOH selectivity (~95%) was maintained; that is, the AQY was independent of the light intensity. The other regime is >5.0 mW cm^{-2}, where the reaction order for the HCOOH rate decreased dramatically, accompanied by more pronounced byproduct formation of H_2. However, a **RuCP** hybrid photocatalyst with a more negative reduction potential showed an $I^{\sim 0.7}$ dependence of CO_2 reduction to HCOOH with 90–95% selectivity in the entire examined light-intensity range. On the basis of these results, we concluded that, in **RuP**/Ag/PCN, light absorption dominates the overall CO_2 reduction rate at $I \leq 5.0$ mW cm^{-2}, whereas CO_2 reduction over **RuP** is the rate-determining step at $I \geq 5.0$ mW cm^{-2}. In **RuCP**/Ag/PCN, electron transfer from PCN to **RuCP** is the bottleneck that determines the overall reaction rate. These results suggest that, under lower light-intensity conditions, molecular catalysts with a more positive reduction potential function better and give a greater reaction quantum yield than those with a more negative potential, although the absolute amount of CO_2 reduction product becomes inevitably low.

Thus far, the development of metal-complex/semiconductor hybrid photocatalysts has relied on the individual refinement of both the metal-complex and semiconductor parts, where CO_2 reduction occurs more quickly/selectively and charge recombination in relation to any back electron transfer reaction is minimal.[6,8] The results of the present work based on the light-intensity dependence clearly provide more general insights into improving the CO_2 reduction performance of metal-complex/semiconductor hybrid photocatalysts.

Experimental

Purification of solvent

DMA and TEOA were distilled before use. The distillation was performed according to our previous work.[31] DMA was dried over 4 Å molecular sieves for several days and distilled under reduced pressure (10–20 torr). TEOA was distilled under reduced pressure (<1 torr). Distilled DMA and TEOA were kept under an Ar atmosphere before use. All other reagents were commercially available and used without further purification.

Synthesis of PCN

PCN samples were synthesized according to a previous method[33] by heating 12.0 g of urea (>99.0%, FUJIFILM Wako Pure Chemical) in air at a ramp rate of 2.2 K min^{-1} to 823 K, maintaining that temperature for 4 h, then cooling without temperature control. Approximately 0.58 g of the PCN powder was obtained.

Synthesis of Ag/PCN

The Ag was loaded in the same manner as in our previous study.[17] Ag species as promoters were loaded onto the surface of PCN by an impregnation method using $AgNO_3$ (>99.8%, Wako Pure Chemicals) as the precursor. PCN was dispersed in an aqueous $AgNO_3$ solution (10 mL). The water content was slowly removed under reduced pressure at room temperature (~298 K) using an evaporator in the dark. The resultant solid sample was heated under a H_2 stream (20 mL min^{-1}) at 473 K for 1 h. The Ag loading amount was 2.0 wt% (nominal value).

Synthesis of RuP and RuCP

Ru complexes (**RuP** and **RuCP**) were synthesized according to the procedures reported by Anderson *et al.*[28] Briefly, Ru polymer $[Ru(CO)_2Cl_2]_n$ was refluxed in ethanol with $(PO_3Et_2)_2$bpy (for **RuP**) or $(PO_3Et_2CH_2)_2$bpy (for **RuCP**) ligands and the obtained powders were refluxed in HCl aqueous solution (4 M) for the hydrolysis to obtain phosphonic (or methylphosphonic) acid anchors.

Adsorption of Ru complex by Ag/PCN

The adsorption of **RuP** (or **RuCP**) was conducted in a manner similar to that previously reported.[17,31,33] PCN was dispersed in methanol containing dissolved **RuP**. The suspension was stirred for 24 h at room temperature (~298 K) in the dark under an Ar atmosphere to allow for adsorption/desorption equilibrium, followed by filtration. The amount of adsorbed **RuP** (or **RuCP**) was calculated on the basis of the UV-vis spectrum of the filtrate. In the present report, the amount of adsorbed Ru complexes was 2 μmol g^{-1}. Typical UV-visible absorption spectra of the solutions before and after the adsorption procedure are shown in Fig. S5.†

Synthesis of Pt/PCN

Pt loading was carried out by impregnation followed by H_2 reduction, similar to the aforementioned method of Ag loading. Pt was loaded onto the PCN using $H_2PtCl_6 \cdot 6H_2O$ (>98.5%, Kanto Chemical) as the precursor. The water was subsequently removed slowly by heating. The resultant solid sample was heated under a H_2 stream (20 mL min^{-1}) at 473 K for 1 h. The Pt loading amount was 2.0 wt% (nominal value).

Photocatalytic reaction

Photocatalytic reactions were performed in a 30 mL Pyrex cuvette containing 14 mL of a mixed solution of DMA and TEOA (4 : 1 v/v) and 14 mg of photocatalyst, which was kept at room temperature using a water jacket. In this study, CO_2 reduction was performed by **RuP**/Ag/PCN (or **RuCP**/Ag/PCN) and H_2 evolution by Pt/PCN. Before irradiation, the suspension was purged with CO_2 (>99.995%, Taiyo Nippon Sanso) for 25–30 min. The light source was a 400 W Xe lamp (Asahi Spectra, MAX-400D) equipped with a bandpass filter ($\lambda = 400$ nm) that allowed the light intensity to be controlled. Some spectral irradiance data are displayed in Fig. S6.† The gaseous reaction products were analyzed using a gas chromatograph equipped with a thermal conductivity detector (GL Science, GC32 or Shimadzu, GC-2014; carrier gas, Ar). The HCOOH generated in the liquid phase was analyzed using a capillary electrophoresis system (Otsuka Electronics, Agilent-7100).

The turnover number (TON) was calculated by the following equation:

$$\mathrm{TON} = \frac{\text{amount of producted HCOOH}(\mu\text{mol})}{\text{amount of adsorbed Ru complex}(\mu\text{mol})}$$

Data availability

The data supporting this article have been included as part of the ESI.†

Author contributions

K. M. designed/supervised the project and wrote the manuscript draft with R. N. and M. O. R. N. conducted photocatalytic reactions and main characterization. J. O. and T. T. synthesized Ru complexes with R. N. C. Z. and G. Z. performed TEM and XPS measurements. All authors reviewed the manuscript and approved its submission.

Conflicts of interest

There are no conflicts to declare.

Acknowledgements

This work was supported by a Grant-in-Aid for Transformative Research Areas (A) "Supra-ceramics" (JP22H05148) and a bilateral collaboration program (JPJSBP120237406) (JSPS). Acknowledgement is also extended to a grant from the National Natural Science Foundation of China (22311540011).

Notes and references

1 J. H. Ye, T. Ju, H. Huang, L. L. Liao and D. G. Yu, *Acc. Chem. Res.*, 2021, **54**, 2518–2531.
2 M. He, Y. Sun and B. Han, *Angew. Chem., Int. Ed.*, 2022, **61**, e202112835.
3 L. Wang, C. Qi, W. Xiong and H. Jiang, *Chin. J. Catal.*, 2022, **43**, 1598–1617.
4 Y. Amao, *Sustain. Energy Fuels*, 2018, **2**, 1928–1950.
5 S. Sato, T. Arai and T. Morikawa, *Inorg. Chem.*, 2015, **54**, 5105–5113.
6 K. Maeda, *Adv. Mater.*, 2019, **31**, e1808205.
7 K. E. Dalle, J. Warnan, J. J. Leung, B. Reuillard, I. S. Karmel and E. Reisner, *Chem. Rev.*, 2019, **119**, 2752–2875.
8 A. Nakada, H. Kumagai, M. Robert, O. Ishitani and K. Maeda, *Acc. Mater. Res.*, 2021, **2**, 458–470.
9 K. Maeda, K. Sekizawa and O. Ishitani, *Chem. Commun.*, 2013, **49**, 10127–10129.
10 J. Lin, Z. Pan and X. Wang, *ACS Sustainable Chem. Eng.*, 2013, **2**, 353–358.
11 R. Kuriki, K. Sekizawa, O. Ishitani and K. Maeda, *Angew. Chem., Int. Ed.*, 2015, **54**, 2406–2409.
12 J. J. Walsh, C. Jiang, J. Tang and A. J. Cowan, *Phys. Chem. Chem. Phys.*, 2016, **18**, 24825–24829.
13 G. Zhao, H. Pang, G. Liu, P. Li, H. Liu, H. Zhang, L. Shi and J. Ye, *Appl. Catal., B*, 2017, **200**, 141–149.
14 C. Cometto, R. Kuriki, L. Chen, K. Maeda, T. C. Lau, O. Ishitani and M. Robert, *J. Am. Chem. Soc.*, 2018, **140**, 7437–7440.
15 S. Roy and E. Reisner, *Angew. Chem., Int. Ed.*, 2019, **58**, 12180–12184.
16 B. Ma, G. Chen, C. Fave, L. Chen, R. Kuriki, K. Maeda, O. Ishitani, T. C. Lau, J. Bonin and M. Robert, *J. Am. Chem. Soc.*, 2020, **142**, 6188–6195.
17 K. Maeda, D. An, C. S. Kumara Ranasinghe, T. Uchiyama, R. Kuriki, T. Kanazawa, D. Lu, S. Nozawa, A. Yamakata, Y. Uchimoto and O. Ishitani, *J. Mater. Chem. A*, 2018, **6**, 9708–9715.
18 N. Sakakibara, K. Kamogawa, A. Miyoshi, K. Maeda and O. Ishitani, *Energy Fuels*, 2024, **38**, 2343–2350.
19 S. Tabata, H. Ohnishi, E. Yagasaki, M. Ippommatsu and K. Domen, *Catal. Lett.*, 1994, **28**, 417–422.
20 T. Torimoto, Y. Aburakawa, Y. Kawahara, S. Ikeda and B. Ohtani, *Chem. Phys. Lett.*, 2004, **392**, 220–224.
21 T. Hisatomi, K. Maeda, K. Takanabe, J. Kubota and K. Domen, *J. Phys. Chem. C*, 2009, **113**, 21458–21466.
22 P. Ketwong, S. Yoshihara, S. Takeuchi, M. Takashima and B. Ohtani, *J. Chem. Phys.*, 2020, **153**, 124709.
23 R. Han, M. A. Melo, Z. Zhao, Z. Wu and F. E. Osterloh, *J. Phys. Chem. C*, 2020, **124**, 9724–9733.
24 K. Maeda, T. Maeda, C. Suppaso, S. Nishioka, Y. Kamakura, S. Yasuda and T. Yokoi, *Sustain. Energy Fuels*, 2024, **8**, 36–42.
25 M. Dilla, A. Mateblowski, S. Ristig and J. Strunk, *ChemCatChem*, 2017, **9**, 4345–4352.

26 W. Shangguan, Q. Liu, Y. Wang, N. Sun, Y. Liu, R. Zhao, Y. Li, C. Wang and J. Zhao, *Nat. Commun.*, 2022, **13**, 3894.
27 Y. Kuramochi, J. Itabashi, K. Fukaya, A. Enomoto, M. Yoshida and H. Ishida, *Chem. Sci.*, 2015, **6**, 3063–3074.
28 P. A. Anderson, G. B. Deacon, K. H. Haarmann, F. R. Keene, T. J. Meyer, D. A. Reitsma, B. W. Skelton, G. F. Strouse and N. C. Thomas, *Inorg. Chem.*, 1995, **34**, 6145–6157.
29 S. Sato, T. Arai, T. Morikawa, K. Uemura, T. M. Suzuki, H. Tanaka and T. Kajino, *J. Am. Chem. Soc.*, 2011, **133**, 15240–15243.
30 Y. Kuramochi, K. Fukaya, M. Yoshida and H. Ishida, *Chem.–Eur. J.*, 2015, **21**, 10049–10060.
31 R. Kuriki, H. Matsunaga, T. Nakashima, K. Wada, A. Yamakata, O. Ishitani and K. Maeda, *J. Am. Chem. Soc.*, 2016, **138**, 5159–5170.
32 K. Maeda, X. Wang, Y. Nishihara, D. Lu, M. Antonietti and K. Domen, *J. Phys. Chem. C*, 2009, **113**, 4940–4947.
33 M. Shizuno, K. Kato, S. Nishioka, T. Kanazawa, D. Saito, S. Nozawa, A. Yamakata, O. Ishitani and K. Maeda, *ACS Appl. Energy Mater.*, 2022, **5**, 9479–9486.

